Iranian Journal of Chemical Engineering
Vol. 9, No. 3 (Summer), 2012, IAChE

Compartment Mixing Model in a Stirred Tank Equipped Dual Rushton Turbine

F. Fakheri, J. Moghaddas[*]
Transport Phenomena Research Center, Chemical Engineering Faculty,
Sahand University of Technology, Tabriz, Iran

Abstract

Knowledge of mixing time is of fundamental importance for investigation of mixing efficiency in agitation systems. The mixing time obtained by using the correlation and formula in large scale mixing systems was incorrect. Again, the number of available correlations in this scale of mixing systems is limited. To predict the mixing time of stirred tanks with dual impellers commonly used in industry, a third-compartment mixing model was used. The time of homogenization of the charge (mixing time) was calculated from the time dependency of the local concentration of tracer measured at various locations. Experimental data on mixing time were obtained with a conductivity technique. In the present study distribution of tracer in the bulk of the liquid was described by compartment model (CM) as well as for stirred vessel with dual Rushton impellers. As for the model, a good agreement between the experimental data and the calculated values was apparent.

Keywords: *Mixing Time, Compartment Model, Rushton Turbine, Tracer, Conductivity*

1. Introduction

Knowledge of mixing time is of fundamental importance for mixing investigation in agitation systems. In fact, this characteristic controls the performance of the mechanically agitated tanks and has a direct influence on the cost of the agitation process [1]. Therefore, mixing time can be used as a comparative measure of the mixer's efficiency, with the same power input. Many attempts, however, have been made over the last 50 years to predict mixing times in stirred tanks [2]. There are two types of overall investigation of the mixing behavior in agitated system: mixing time from experimental measurements and the results from the simulation studies. For the mixing time measurements several models to approach the homogenizing process have been proposed, e.g., the circulation model, the eddy diffusion model, the zone network model, the CFD model and the compartment model. These models are developed based on the three mechanisms of the molecular diffusion, the eddy diffusion and bulk convection [3–5].

* Corresponding author: Jafar.moghaddas@sut.ac.ir

2. Structure of the compartment model

Compared to single impeller arrangements, the flow within tall vessels stirred with multiple impellers is more complex. Stirred vessel equipped with dual Rushton turbines generate three distinctly different stable flow patterns depending on the off-bottom clearance of the lower impeller and the spacing between the two impellers [5, 6]. These flow patterns are defined as parallel, merging and diverging flow patterns depending upon the interaction of the liquid circulation loops with each other. When the impeller spacing is 1.2 times greater than the impeller diameter, the flow pattern generated is horizontal and parallel [7]. The flow structure created by dual Rushton turbine in an aerated stirred tank consists of circulation flow, exchange flow and induced flow [8]. The structure and parameter of the hydrodynamic model is shown in Fig. 1. According to the compartment structure in Fig. 1, 2×3 compartments for the impeller zones were used. To investigate the influence of radial distances of the tracer addition points and also to increase the accuracy of the model, a large number of compartments in the radial distance should be used.

3. Determination of model parameters

Circulation flow

Circulation inside the tank is promoted by the turbine pumping capacity Q_P. It should be calculated by integrating the radial-velocity profile and multiplying this by the corresponding area. Experimental measurements confirm that Q_P is proportional to ND^3 in turbulent agitation [5, 9].

$$Q_P = K_P N D^3 \tag{1}$$

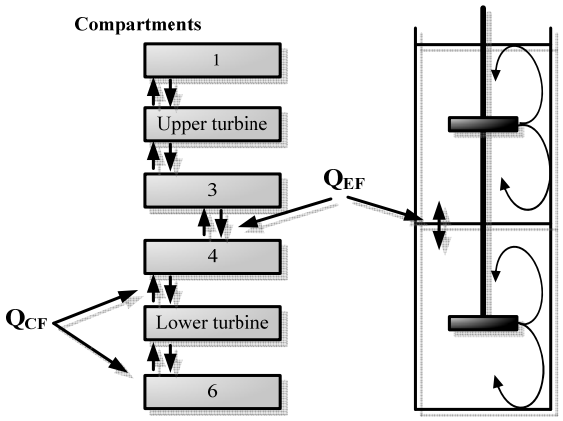

Figure 1. Compartment model Scheme of a two-staged tank

The flow number K_P is the principal dimensionless group. The value of K_P was found to depend on impeller geometry [5, 9]:

$$K_P = 6.2\left(\frac{W}{D}\right)\left(\frac{D}{T}\right)^{0.3} \tag{2}$$

$$K_P = 0.21\left(\frac{T}{D}\right)^{1.8} \tag{3}$$

Mahouast et al. found the circulation flow rate is usually considered to be twice the impeller pumping capacity at the front of the impeller [10]. Cui et al. therefore argued that the average circulation flow rate in the whole path should be used [5]. That rate was assumed to be 80% of the value given by Eq. 1 [3, 5].

$$Q_{CF} = K_{CF} N D^3 \qquad K_{CF} = 2 \times 0.8 \times K_P = 1.2 K_P \tag{4}$$

4. Exchange flow

The exchange flow rate describes the Interchange flow between adjacent stages in the axial direction. For the stirred tank, in the fully turbulent regime and for the full range

of Newtonian working fluids the characteristic turbulent velocity and length scales are [3, 5, 11]

$$u_c = C_u' V_{TIP} = C_u ND$$
$$L_c = C_L D \quad (5)$$

The constants C_u and C_L are a function of the impeller and tank geometry selected. The dissipation, ε, is the rate of dissipation of turbulent kinetic energy. The turbulent kinetic energy must scale with u_c^2. The rate of dissipation of energy is taken to scale with u_c / L_c, the characteristic time scale of the flow. This gives

$$\varepsilon \propto \frac{u_c^3}{L_c} \quad (6)$$

For isotropic turbulent flow, the root mean square fluctuation velocity of containing eddies can be calculated by Eq. 6 [3, 5].

$$u_c = (L_c \varepsilon)^{1/3} \quad (7)$$

A second estimate of turbulence characteristics which avoids the need for C_u is the power per unit mass of fluid in the tank [5].

$$\varepsilon = \frac{P}{\rho V_{Tank}} = \frac{4 N_P \rho N^3 D^5}{\rho \pi T^2 H_i} \quad (8)$$

The combination of Eq.7 with Eq.5 and 8 gives Eq. 9 [3, 5].

$$u_c = K_Z' N_P^{1/3} N D^2 (T^2 H_i)^{-1/3} \quad (9)$$

The exchange flow rate can be calculated from Eq.9 with $K_Z = \pi K_Z' N_P^{1/3} / 4$ [3, 5]

$$Q_{EF} = \bar{u}_Z' \pi (\frac{T}{2})^2 = K_Z N D^3 [(\frac{T}{D})^{4/3} (\frac{H_i}{D})^{-1/3}] = K_{EF} N D^3 \quad (10)$$

K_{EF} is a fraction coefficient of the flow in axial direction induced by an impeller and is proportional to the pumping capacity and the dimensionless geometry factor of a stirred tank. The dimensionless inter-stage exchange flow number for similar stirred tank is consistent with the value 0.59 reported by Alves and Vasconcelos and matches the prediction of 0.6-0.7 for tanks of 0.3-0.5 m diameter, according to Vasconcelos et al. [9]. From the measure of the axial exchange flow rate reported in the literature for Rushton turbines, the following relationship was found between K_{EF} and T/D.

$$K_{EF} = b \frac{T}{D} \quad (11)$$

where b is 0.194 in the small tank and 0.236 in the large tank (95% confidence interval) [9].

5. Induced flow

Besides the axial turbulent liquid exchange and circulation flow, an extra flow pattern induced by air bubbles was found as a consequence of the density difference in an aerated agitated tank. This flow is dependent on the gas flow rate and pumping capacity [3, 12], thus in the liquid mixing system Induced flow is negligible.

6. Experimental

The experimental setup is shown

schematically in Fig. 2. All experiments were carried out in a transparent vessel with a flat bottom, having an inner diameter, T, of 0.3m. The cylindrical tank body was made of glass and working heights liquid was 0.54 m. The stirred tank was fitted with four wall mounted baffles having a width of 1/10th and thickness 1/100th that of the tank diameter (fully baffled condition). Two six – bladed Rushton turbine impellers with a diameter of D=T/3 were placed in the tank. The impeller width, L, and the impeller blade height, W, were equal to D/4 and D/5. The off – bottom clearance is C_1=0.55T, and the upper impeller is placed ΔC=0.7T above the lower one. The stirred tank is filled with tap water as the main continuous phase fluid, the surface of which is C_2=0.55T above the upper impeller. A pump drives the turbines and the stirring speed is measured using a calibrated digital oscilloscope. A tachometer was used to measure the impeller speed for certitude. For measuring the mixing time a small quantity of tracer (60 ml of NaCl solution (100 g/L)) is added on the top of the dispersion surface and 11 ports were used for tracer detection. The coordinates of these positions are listed in Table 1.The mixing time was estimated for each of the probes as the time required to attain the final concentration within ±5% of the average concentration.

7. Results and discussion

In the present paper, a CM was adopted in which the vessel is theoretically divided into three compartments per stage in the other two mixers corresponding to the number of impellers, in which zones 3 and 4 have the same condition of flow characteristic affected by velocity vector. Since the tracer with a certain amount of volume and concentration was injected into the vessel, bulk convection mechanism is used in the homogenizing process.

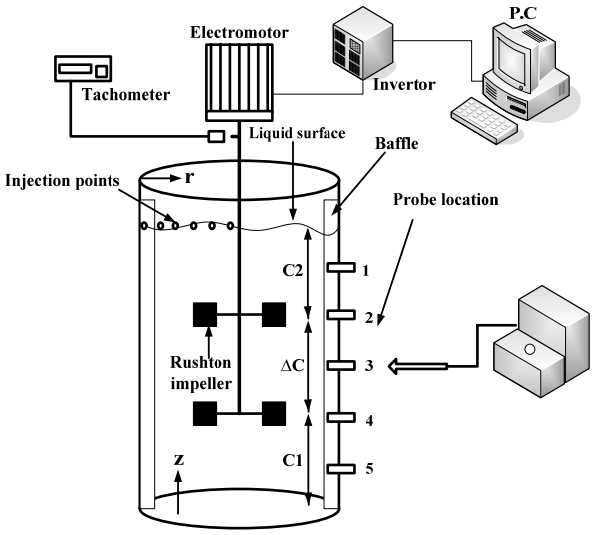

Figure 2. Schematic of the experimental set and details of the tank

Table 1. Positions of detectors and injection point

Position	Injection points		Probe locations	
	R	(r/T)	Z (cm)	(z/H)
1	1.5	0.05	47.75	0.847
2	2.5	0.083	37.5	0.690
3	3.5	0.117	27	0.5
4	4.5	0.15	16.5	0.305
5	5.5	0.183	8.25	0.153
6	6.5	0.217	-	-
7	7.5	0.25	-	-
8	8.5	0.283	-	-
9	9.5	0.317	-	-
10	10.5	0.35	-	-
11	12.5	0.383	-	-

To verify the model, the theoretically predicted concentration curves which are

obtained by the tracer concentration in several locations can be compared with those obtained by experiment. Concentration transients were simultaneously solved by the numerical solution of the system of ordinary differential equations which obtained the transient mass balance of the tracer in each compartment [3, 5, 8, 9].

$$
\begin{aligned}
V_1\frac{dC_1}{dt} &= Q_{in}C_{in} + Q_{IF}C_2 - Q_{IF}C_1 + Q_{CF}C_2 - Q_{CF}C_1\\
V_2\frac{dC_2}{dt} &= Q_{CF}C_3 + Q_{CF}C_1 - 2Q_{CF}C_2 + Q_{IF}C_3 + Q_{IF}C_1\\
&\quad - 2Q_{IF}C_2\\
V_3\frac{dC_3}{dt} &= Q_{IF}C_4 + Q_{IF}C_2 - 2Q_{IF}C_3 + Q_{EF}C_4\\
&\quad - Q_{EF}C_3 + Q_{CF}C_2 - Q_{CF}C_3\\
V_4\frac{dC_4}{dt} &= Q_{IF}C_5 + Q_{IF}C_3 - 2Q_{IF}C_4 + Q_{EF}C_3\\
&\quad - Q_{EF}C_4 + Q_{CF}C_5 - Q_{CF}C_4\\
V_5\frac{dC_5}{dt} &= Q_{CF}C_4 + Q_{CF}C_6 - 2Q_{CF}C_5 + Q_{IF}C_4\\
&\quad + Q_{IF}C_6 - 2Q_{IF}C_5\\
V_6\frac{dC_6}{dt} &= Q_{IF}C_5 - Q_{IF}C_6 + Q_{CF}C_5 - Q_{CF}C_6
\end{aligned}
\qquad (12)
$$

where V_i is volume of each compartment and C_i represents the tracer concentration in the *i*th compartment. This system of first-order differential equations was solved by Runge-Kutta fourth order method. The initial values are computed with the knowledge of the volume and concentration of the tracer injected into the vessel. It was assumed that, after injection at time t = 0, the concentration C_1 prevails; and no tracer concentration would be present in the other compartments (assumption of ideal mixing) [3, 8, 9]. In order to obtain mixing time, it is necessary to understand the model parameters. Computed exchange flow rate (Q_{EF}) and circulation flow rate (Q_{CF}) between the compartments are shown in Table 2. The parameters of the model were computed by Moghaddas et al. from experimental data [13] and the Eq. 11 [9]. The results obtained from previous information confirm the high accuracy of Eq. 11 and Moghaddas' et al. data, rather than Eq. 2 and 10.

Table 2. Exchange and circulation flow rate between the compartments

	Model parameter (m^3/s)	**300 RPM**	**400 RPM**
Moghaddas (2004) [13]	Q_{CF}	5.22×10^{-3}	7.36×10^{-3}
by Eq. 2	Q_{CF}	5.34×10^{-3}	7.12×10^{-3}
by Eq. 11	Q_{EF}	3.54×10^{-3}	4.72×10^{-3}
by Eq. 10	Q_{EF}	3.15×10^{-3}	4.2×10^{-3}

The effect of different situation measurements of the tracer concentration on the mixing time by using CM is shown in Fig. 3(a). It is obvious that the situation measurements of the tracer concentration, being far from the injection point, decreased the intensity of the peak. Fig. 3(b) shows the comparison between the measured and calculated curves of the concentration profiles and indicates that the model accurately describes the behavior of a real mixed system.

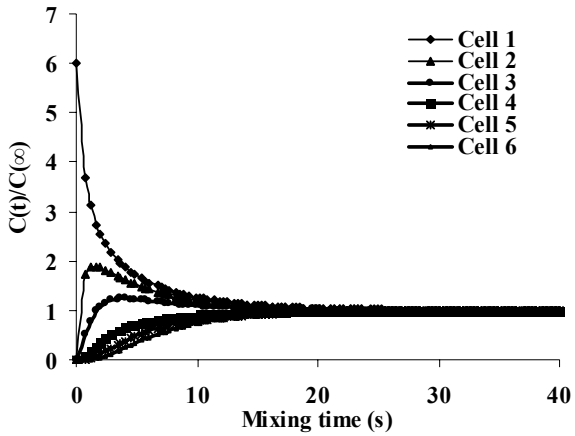

(a)

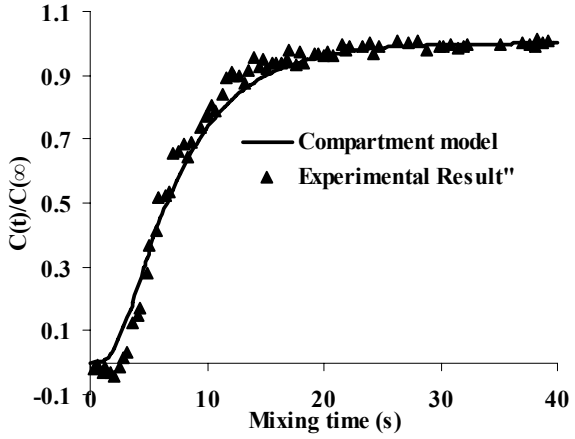

(b)

Figure 3. (a). Response curves calculated from CM (b). Comparison of experimental response curve and that calculated from CM

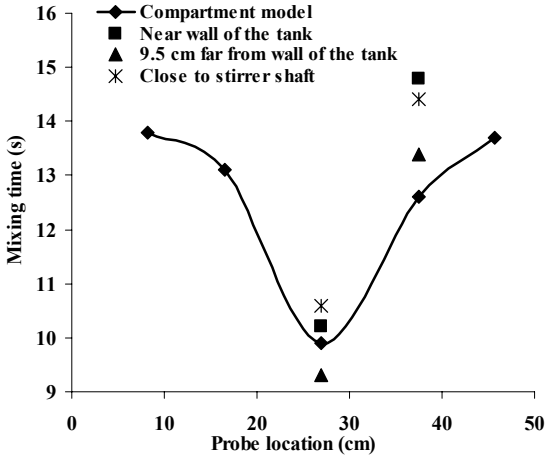

(a)

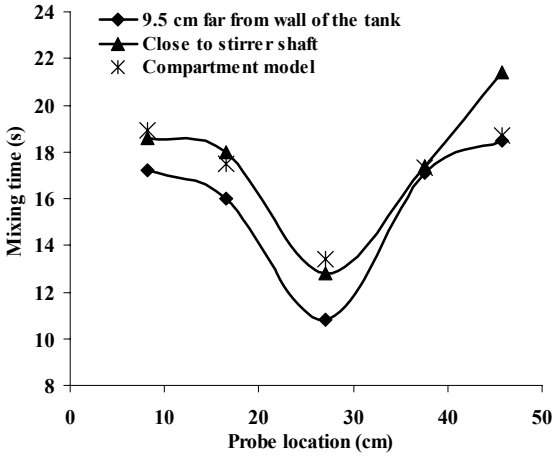

(b)

Figure 4. Effect of different situation measurements of the tracer concentration on the mixing time: (a) 400rpm, (b) 300 rpm.

In the region between the upper and lower impellers, the radial pumping flow rate increased. In this region homogenization of the liquid was done by both upper and lower circulation flow rate. The results of circulation loops turn back a higher volume of the liquid to the back of the blade. This caused the mixing time resulted from position three and four to be lower than the other position. The result from CM shows the effect of different situation measurements of the tracer concentration on the mixing time, at first decreased and then increased. The maximum mixing time obtained was from region one and six. In the experimental work, three tracer injection points on the liquid surface were supposed (neighbor to wall of the tank, 9.5 cm far from wall of the tank and close to stirrer shaft). Mixing times obtained from the compartment model for 400 rpm have a good agreement with location of the tracer injection at 9.5 cm far from wall of the tank. Average deviations of experimental

data at the 300 rpm for the location of the tracer injection at 9.5 cm far from the wall of the tank and close to stirrer shaft are +7.9% and -2.3% respectively. Experimental results show that the effect of tracer injection point at the liquid surface on the mixing time was negligible. Therefore, the mixing time computed from CM in the radial distances was from the stirrer shaft to 9.5 cm far from the wall of the tank.

8. Conclusions

In this work, the compartment model was used for the calculation of mixing time ($t_{95\%}$) in single phase stirred tanks by dual Rushton turbines. A good agreement between the time dependence of the concentration obtained experimentally and that calculated from theory was obtained. The result from CM shows the effect of different situation measurements of the tracer concentration on the mixing time first decreased and then increased.

Nomenclature

H	Liquid height (m)
T	tank diameter(m)
D	impeller diameter(m)
W	impeller blade height(m)
L	impeller blade width(m)
ΔC	impeller spacing(m)
C_1	off bottom clearance of the lower turbine(m)
N	impeller rotational speed (rpm)
Q_P	pumping capacity (m^3/s)
Q_{CF}	circulation flow rate (m^3/s)
Q_{EF}	exchange flow rate (m^3/s)
Q_{IF}	induced flow rate (m^3/s)
C_i	tracer concentration in the *i*th compartment (gr/lit)
C(t)	tracer concentration at time t (gr/lit)
$C(\infty)$	final tracer concentration (gr/lit)
N_P	power number (-)
ε	turbulent kinetic energy dissipation rate (m^2/s^3)
u_c	characteristic turbulent velocity scale (m/s)
L_c	characteristic length scale (m)
Q_{in}	volumetric tracer flow rate (m^3/s)
C_{in}	tracer concentration (gr/lit)
Hi	denotes compartment height (m)
V_{TIP}	Impeller tip velocity (m/s)
V_i	denotes compartment volume (m^3)

References

[1] Houcine, I., Plasari, E., and David, R., "Effects of the stirred tank's design on power consumption and mixing time in liquid phase", Chem. Eng. Technol., 23, 605–613, (2000).

[2] Guillard, F. and Tragardh, C., "Mixing in industrial Rushton turbine-agitated reactors under aerated conditions", Chem. Eng. and Proc., 42, 373–386, (2003).

[3] Vrabel, P., Van Der Lans, R., Cui, Y.Q., Luyben, K. and Ch, A.M., "Compartment model approach: Mixing in large scale aerated reactors with

multiple impellers", Chem. Eng. Res. Des., 77, 291–302, (1999).

[4] Hiraoka, S., Tada, Y., Kato, Y., Matsuura, A., Yamaguchi, T. and Lee, Y.S., "Model analysis of mixing time correlation in an agitated vessel with paddle impeller", J. Chem. Eng. Jpn., 34, 1499-1505, (2001).

[5] Cui, Y.Q., Lans, R., Noorman, H.J. and Luyben, K., "Compartment mixing model for stirred reactors with multiple impellers", Chem. Eng. Res. Des., 74, 261-271, (1996).

[6] Shewale, S.D. and Pandit, A.B., "Studies in multiple impeller agitated gas-liquid contactors", Chem. Eng. Sci., 61, 489-504, (2006).

[7] Khopkar, A.R. and Tanguy, P.A., "CFD simulation of gas-liquid flows in stirred vessel equipped with dual Rushton turbines: Influence of parallel, merging and diverging flow configurations", Chem. Eng. Sci., 63, 3810-3820, (2008).

[8] Kasat, G.R. and Pandit, A.B., "Mixing time studies in multiple impeller agitated reactors", Can. J. Chem. Eng., 82, 892-904, (2008).

[9] Vasconcelos, J.M.T., Alves, S.S. and Barata, J.M., "Mixing in gas-liquid contactors agitated by multiple turbines", Chem. Eng. Sci., 50, 2343-2354, (1995).

[10] Mahouast, M., Fontaine, P. and Mallet, J., "A two compartment LDV bench for automated determination of flow rate and energy transfer generated by agitators", Proceedings of the 7th European Conf. on Mixing, BHRA, Brugge, pp. 181-185, (1991).

[11] Edward, P.L., Atiemo-Obeng, V.A. and Kresta, S.M., Handbook of industrial mixing: science and practice, Hoboken, NJ, John Wiley & Sons, (2004).

[12] Vasconcelos, J.M.T., Alves, S.S., Nienow, A.W. and Bujalski, W., "Scale-up of mixing in gassed multi-turbine agitated vessels", Can. J. Chem. Eng., 76, 398-404, (2009).

[13] Moghaddas, J. S., Tragardh, C., Ostergren, K. and Revstedt, J., "A comparison of the mixing charac-teristisc in single-and two – phase grid-generated turbulent flow systems, Chemical Engineering & Technology, 27(6), 662-670, (2004).